

Measuring Devices Based on Molecular-Electronic Transducers

A. S. Bugaev^{a, b}, A. N. Antonov^{a, c}, B. M. Agafonov^{a, d}, K. S. Belotelov^d, S. S. Vergeles^{a, e},
P. V. Dudkin^a, E. V. Egorov^{a, d}, I. V. Egorov^{a, d}, D. A. Zhevnenko^{a, f, g}, S. N. Zhabin^a,
D. L. Zaitsev^{a, c, d}, T. V. Krishtop^g, A. V. Neeshpapa^{a, d}, V. G. Popov^{a, h},
V. V. Uskov^a, A. S. Shabalina^{a, d}, and V. G. Krishtop^{g, h, *}

^aMoscow Institute of Physics and Technology (State University), Dolgoprudnyi, Moscow oblast, 141700 Russia

^bKotel'nikov Institute of Radio Engineering and Electronics, Russian Academy of Sciences, Moscow, 125009 Russia

^cNordLab LLC, Dolgoprudnyi, Moscow oblast, 141700 Russia

^dR-sensors LLC, Dolgoprudnyi, Moscow oblast, 141701 Russia

^eLandau Institute of Theoretical Physics, Russian Academy of Sciences, Chernogolovka, Moscow oblast, 142432 Russia

^fAO Molecular Electronics Research Institute, Zelenograd, 124460 Russia

^gSeismotronics LLC, Moscow, 141700 Russia

^hInstitute of Microelectronics Technology and High Purity Materials, Russian Academy of Sciences, Chernogolovka, Moscow oblast, 142432 Russia

*e-mail: vgkvgk@mail.ru

Received June 26, 2017

Abstract—The basic principles of operation of the sensors based on molecular-electronic transducers (METs) are described. The review of investigations of physical processes into MET and their operating characteristics are considered. Modern MET manufacturing technologies and the production methods and the new applications of planar microelectronic METs are discussed. An overview of devices and systems based on the METs is given.

DOI: 10.1134/S1064226918110025

INTRODUCTION

Devices based on molecular-electronic transducers (METs) have found wide application in mechanical signal detectors [1–3].

MET-based devices have no high-precision mechanics elements, but, at the same time, they are characterized by a high efficiency of transformation of a mechanical signal into an electric current at a level of physical processes occurring in METs rather than with the help of correcting electronics. Hence, their characteristics are an order of magnitude better than parameters attainable by microelectromechanical systems (MEMSs). Owing to these unique qualities, MET-based devices also compete successfully with more expensive precise electro- and magnitomechanical equipment because their weight is substantially smaller and the cost is less by an order of magnitude. Moreover, METs are undemanding to transportation conditions, almost instantly reaches an operating mode, have a long performance period, and are extremely simple in operation.

At present, in the level of intrinsic noises at high frequencies, MET-based devices are still at a disadvantage in relation to the best electro- and magnitomechanical models. Upon comparison with MEMSs,

their drawbacks are, firstly, an insufficiently high upper cutoff frequency of no more than 3 kHz (however, this is typical of the majority of relatively slow up-to-date electrochemical systems) and, secondly, the greater (by an order of magnitude) cost. Since microelectronic technology of MET manufacturing is constantly developed, these problems should be solved to a considerable degree.

1. PHYSICAL PRINCIPLES OF OPERATION OF THE MOLECULAR-ELECTRONIC TRANSDUCER

Different binary electrolytes ensuring reversible redox reactions, e.g., iodine–iodide, ferri-/ferrocyanide, and so forth, can be used in transducers. In this case, MET electrodes are produced from metals implementing electron exchange, rather than cation one. Theoretically, this enables infinitely long operation of the device without variations in working parameters.

At present, iodine–iodide systems with platinum electrodes have found wide application. An electrolyte of the given system is composed of a high-concentration aqueous solution of potassium iodide (KI) or lith-

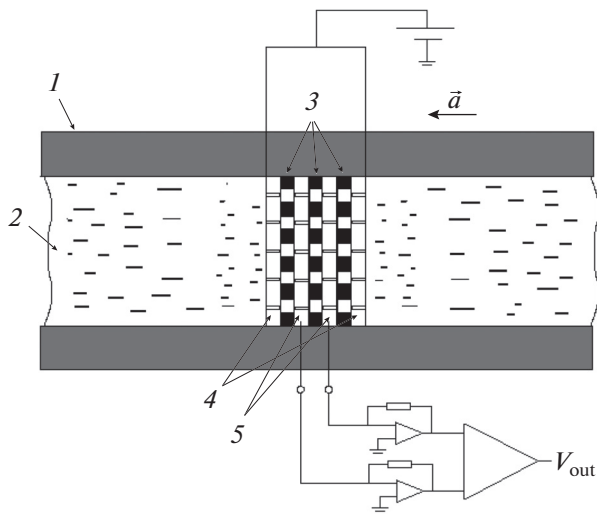


Fig. 1. Typical MET: (1) ceramic or glass tube, (2) electrolyte, (3) porous ceramic partition, (4) anodes, (5) cathodes, \vec{a} is the external mechanical acceleration, and V_{out} is the output signal.

ium iodide (LiI), the lower temperature limits of which are, respectively, -15 and -55°C , and a small amount of molecular iodine (I_2). When iodide is in excess, iodine generates a well soluble complex compound, triiodide, according to the scheme



Upon current passage through any MET, electrochemical reactions by which iodine is reduced at the cathode, namely,



and oxidized at the anode:



occur on its electrodes. Under the above conditions, potassium ions playing the role of a background electrolyte do not participate in reactions.

Typical MET structure is presented in Fig. 1. MET operation relies on the fact that electric current through the MET is determined very largely by hydrodynamic electrolyte motion caused by an external action of mechanical disturbances. The rate of a chemical reaction on MET electrodes considerably exceeds the rate of reactant delivery to them. In this case, during reactions proceeding in the MET, reactant concentration gradient arises and charge transfer within an immovable electrolyte is carried out due to molecular diffusion from one electrode to another. When liquid moves under the action of inertia forces, molecular diffusion is accompanied by convective ion transfer. As result, the rate of reactant delivery to electrodes is abruptly changed and, accordingly, the current flowing through the MET is varied (see Fig. 2).

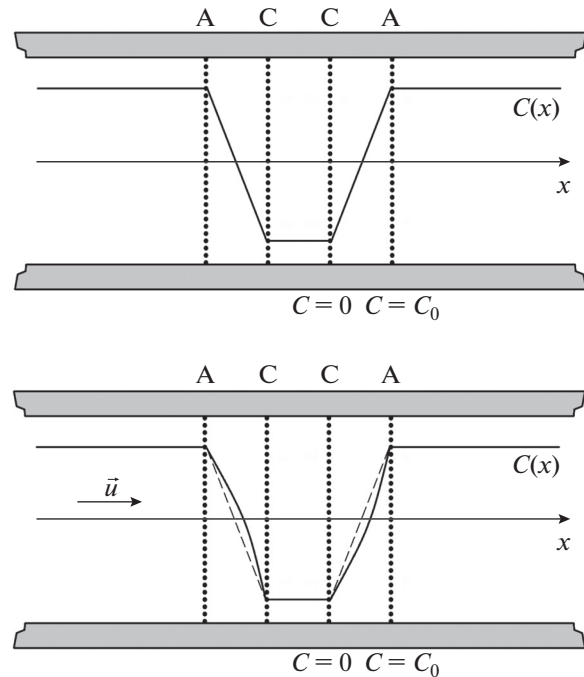


Fig. 2. Electrolyte concentration distribution over an electrode assembly with planar permeable electrodes. The upper figure presents concentration $C(x)$ obtained under the bias voltage. The lower figure illustrate variations in the distribution of concentration $C(x)$ under the action of an incoming liquid flow with velocity is u . Here, C_0 is the equilibrium electrolyte concentration.

Here and in subsequent figures, letters A and C designate an anode and cathode, respectively, and \vec{u} is the electrolyte flow velocity. Modern METs possess a linear output signal relative to acceleration in wide frequency range and under dynamical conditions.

The MET principle of operation can be easily explained using the approximation of planar electrodes permeable to liquid and impermeable to charges, which was first proposed in [4].

Upon exposure to electric voltage, an electrochemical current (so-called "background current") independent of mechanical motion traverses the system (see the upper figure). In this case, electrochemical reactions create the concentration gradient of solution components, and charge transfer is implemented with the help of ion diffusion from one electrode to another.

In the presence of a mechanical signal, an electrolyte begin to move under the action of inertia forces and additional convective ion transport to electrodes is formed together with diffusion, drastically changing the rate of reactant delivery to electrodes and consequently the current passing through a sensing element. The electric current additional to the background one

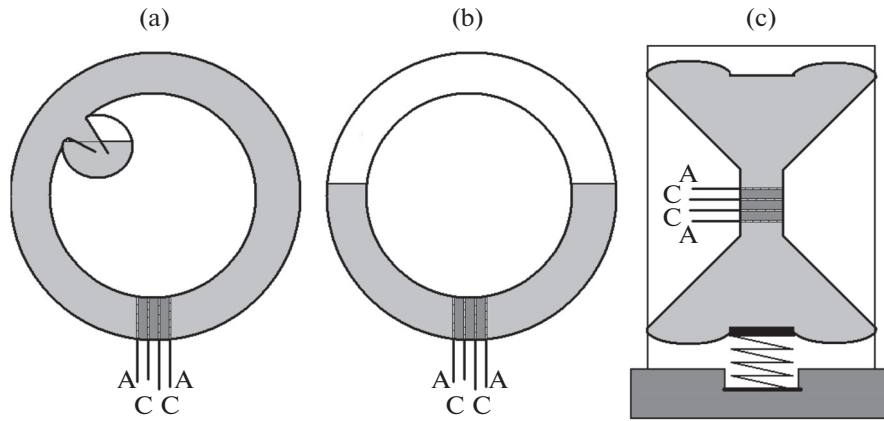


Fig. 3. Types of MET-based sensors: (a) rotational, (b) horizontal, and (c) vertical sensors, A are anodes, and C are cathodes.

and proportional to an external mechanical signal arises in the system.

In other words (see the lower figure), a liquid flow induced by mechanical motion distorts the steady-state distribution of the charge-carrier concentration in an interelectrode space, leading to strong variations in concentration gradient near an electrode surface. In turn, an electric current flowing through the electrode depends on the concentration gradient near its surface as

$$I = -Dq \oint_S (\nabla C \cdot d\vec{s}), \tag{4}$$

where I is the current passing through the electrode, D is the ion diffusion coefficient, q is the single ion charge, and C is the ion concentration (integration is performed over electrode surface S).

The difference-cathode-current amplitude is most often chosen to be an output signal of the four-electrode system incorporating two anodes and two cathodes:

$$I(t) = I_{C_2}(t) - I_{C_1}(t) = Dq \left(\int_{K_2} \vec{n} \cdot \nabla C(t) - \int_{C_1} \vec{n} \cdot \nabla C(t) \right), \tag{5}$$

where t is the time, $I(t)$ is the output signal, and $I_{C_1}(t)$ and $I_{C_2}(t)$ are the currents through cathodes C_1 and C_2 , respectively. In this case, such an apparently simple system is extremely sensitive to mechanical actions by today's standards.

In manufacturing of a seismic sensor, a sensing element is inserted across a dielectric channel restricted by flexible membranes on both sides and filled with a working liquid. The schematic representations of the various sensors are depicted in Fig. 3. The frequency response of a commercial transducer is presented in Fig. 4. The subsequent formation of an output characteristic is achieved with the help of correcting elec-

tronics. Depending on electronic-data processing, it is possible to obtain the output proportional to a velocity (an MTSS-1001/3 velocimeter) or an acceleration (an MTSS-1033 accelerometer). As a result, for, e.g., a velocity sensor, the frequency response has a typical planar shape in the wide frequency range.

Despite rather high output parameters, developed and currently fabricated devices possess several drawbacks limiting the field of their application. The main drawbacks can be formulated as follows:

- (i) The high manufacturing cost of transforming components.
- (ii) The sufficiently strong spread of the parameters of hand-build transforming components. Hence, the concomitant electronics of each sensor had to be adjusted individually, thereby increasing the device cost.
- (iii) The early recession of sensitivity at high frequencies.

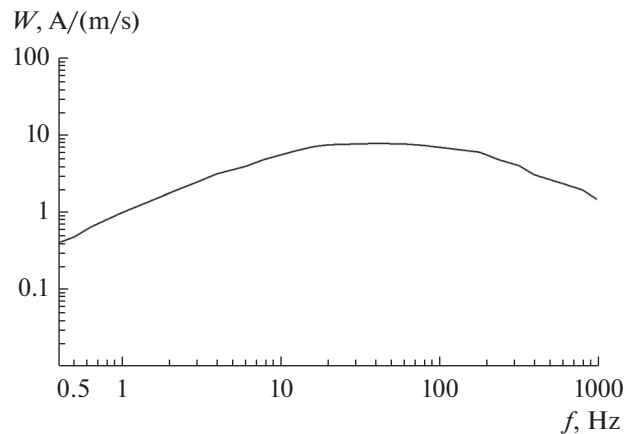


Fig. 4. Frequency response $W(f)$ of the sensing element of a seismosensor with a mesh-type transforming cell.

However, the development of microelectronics production technologies opens up the substantial opportunity of surmounting these problems. It was demonstrated [5–8] that a planar sensing element can be implemented by microelectronic instrumentation. The authors of [8] reported the technological foundations of manufacturing of planar METs.

2. CHARGE AND MASS TRANSFER IN THE MOLECULAR-ELECTRONIC TRANSDUCER

To describe signal transfer and its transformation and calculate frequency, dynamic, and noise characteristics of METs, the system of hydrodynamic and convective-diffusion equations must be solved under conditions of variable electrolyte flow through an electrochemical cell.

The most widespread approach [9–18] to simulation relies on the convective-diffusion equation for I_3^- ions:

$$\frac{\partial C}{\partial t} = D\Delta C - \vec{V} \cdot \vec{\nabla} C, \quad (6)$$

where C is the active ion concentration and \vec{V} is the hydrodynamic electrolyte-flow velocity with respect to a transducer housing. An advantage of the given approach is a simple mathematical formulation of the problem making it possible to obtain analytical solutions [4, 11, 12, 19] or establish nonrigid requirements to computational resources with the help of numerical methods [14, 9, 10, 20–23].

The electrolyte-flow velocity distribution needed to solve (5) can be derived from the Navier–Stokes equation (in calculations of linear responses, it is sufficient to use the approximation of small Reynolds numbers) and the liquid incompressibility condition:

$$\frac{\partial \vec{V}}{\partial t} = \nu \Delta \vec{V} - \frac{\nabla P}{\rho}, \quad (7)$$

$$\operatorname{div} \vec{V} = 0, \quad (8)$$

where ν is the electrolyte viscosity coefficient, p is the pressure, and ρ is the electrolyte density.

The boundary conditions for (7) and (8) are formulated using requirements to “adhesion” to solid surfaces and conditions to the pressure and velocity at the edges of a transforming channel, which are standard for hydrodynamics. After the hydrodynamic-velocity distribution is found, it remains to calculate the ion transfer in the cell and determine electric currents flowing through electrodes.

At small electrolyte-flow velocities, the solution to the convective-diffusion equation can be sought as a series in which each subsequent summand is proportional to electrolyte-flow-velocity amplitude \vec{u} in the higher power. Investigating the system’s linear

response, we can restrict ourselves to the first two terms of expansion:

$$C = C_0 + C_1 \exp(i\omega t), \quad (9)$$

where C_0 is the concentration distribution in a fluid at rest and C_1 is a small additive to the concentration, which is linear with respect to the hydrodynamic velocity and varies according to a harmonic law. Thus, equation (6) is transformed to the following system:

$$\Delta C_0 = 0, \quad (10)$$

$$\frac{\partial C_1}{\partial t} = D\Delta C_1 - \vec{V} \cdot \vec{\nabla} C_0. \quad (11)$$

In the linear approximation, the system involving Eqs. (7), (8), (10), and (11) the convective-diffusion processes occurring in the cell are fully determined by. As a rule, the boundary conditions employed during its solution are the natural physical conditions under which active ion flows are lacking on dielectric surfaces and their concentration on conducting electrodes is fixed, the requirements to the constancy of liquid adhesion at solid walls (they are standard for hydrodynamics), and the conditions of pressure gradient at the input and output channels of a transforming component. In finding the I_3^- -ion concentration on electrodes, the boundary condition of limiting current or the Nernst equation are employed as the boundary condition.

For a practically used transforming cell, the I_3^- -ion concentration is chosen in the range of 0.01–0.1 mol/L. In this case, ions belonging to KI have an appreciably higher concentration (it value varies from 2 to 4 mol/L). As was revealed in [24, 27], it is possible to introduce the small parameter $\varepsilon \sim C_{I_3^-}/C_b \sim \delta C_{I^-}/C_b \sim \delta C_{K^+}/C_b$, where $\delta C_{I^-} = C_{I^-} - C_b$, $\delta C_{K^+} = C_{K^+} - C_b$, and C_b is the potassium iodide concentration in a homogeneous solution.

Equation (6) is most often solved using the simplified boundary conditions [24] comprising the requirement to the constancy of the concentration of electroactive I_3^- ions [7, 8, 18–21, 25] and the condition of the constancy of the current density on electrode surfaces [16–18, 26, 27]. In the cases where the interelectrode distance exceeds diffusive and hydrodynamic lengths in the system, electrodes can be interpreted to be distant from each other. Therefore, the conditions on distant anodes weakly affect simulation data on cathode currents forming an output signal. Moreover, for the limiting current mode employed in real sensors, the condition concerning the zero concentration of major ions on the cathode surface is well-founded (in the case of iodine–iodide systems, the zero concentration condition on the cathode refers to I_3^- ions). In connection with this, when simplified boundary conditions were applied to such systems, the obtained theoretical

dependences turn out to be in good agreement with experimental results.

3. MOLECULAR-ELECTRONIC TRANSDUCER MODELS

Charge transfer in the molecular-electronic cell is simulated with the aim of calculating electrode currents under steady-state conditions and in the case where liquid moves due to inertia forces. This enables us to find the transforming-cell response at the specified type of mechanical actions.

Early theoretical models were commonly employed to investigate a simplified 1D problem [1, 4, 28, 29]. In the context of such models, calculations provided unsatisfactory conformity with experimental data. With the help of analytical and numerical methods, theoretical models were developed for certain configurations close to existing electrode systems [9–18] (see Fig. 3). In particular, it was demonstrated [13] that the transforming-cell geometry being a rather complex 3D structure must be successively taken into account.

It should be noted that the majority of previously developed theoretical models operate mainly at low frequencies (from thousandths to several hertz). In particular, a practical value of these models is related to wide application of MET-based sensors in long-period seismology. The new theoretical models had to be developed to create micro- and nanotransducers. Hence, many works devoted to the study of transfer processes in METs with different configurations and investigations into the characteristics of the given transducers have been performed both at low and infralow frequencies [30–33] and in the high-frequency spectral region [11, 12, 16, 17, 34]. From the viewpoint of the output parameters of a sensing element, basic drawbacks of seismosensors are associated with the special behavior of its characteristics at high frequencies.

Sensing-element miniaturization [12] promotes a substantial increase in the upper operating frequency of METs. However, a further decrease in sizes is possible only with the help of microelectronic technologies [6, 7].

Owing to the development of microelectronic technology of the manufacturing of MET electrode assemblies with the help of standard microelectronic technologies, not only an electrode assembly but also the transducer-parameter spread can be considerably miniaturized, energy consumption is diminished, and the cost of fabricated sensors can be appreciably reduced. An electrode system with planar electrodes has a number of advantages over other discussed configurations of electrodes even if the characteristic configurations of transforming microstructures are preserved at the previous level. Since the typical sizes of the basic components of a transforming system can be

decreased, it is possible to extend the transducer's frequency range, increase the linearity, and, in many cases, ensure the higher sensitivity. In this case, an important parameter of the planar structure, which largely determines planar MET characteristics, is the distance between a cathode and an anode.

A principal novelty consists in that micro- and nanotechnologies of MET production can diminish the typical size of main structural components down to 100 nm, i.e., can provide a decrease by 2–3 orders of magnitude in the characteristic sizes of transforming components achievable due to modern technologies. A substantial decrease in transforming-component sizes can radically enhance the technical parameters of sensors on their basis.

4. NOISES IN THE MOLECULAR-ELECTRONIC TRANSDUCER AND GENERAL REGULARITIES

The main mechanism of MET noises is caused by hydrodynamic fluctuations of a liquid flow through a transforming cell. It was experimentally ascertained that the noise mechanism is determinative for METs at frequencies lower than several hertz. Balanced hydrodynamic fluctuations in models corresponding to real molecular-electronic seismosensors were discussed in [35]. The fluctuation-dissipation theorem made it possible to derive the expression for the spectral density of the mean square of a pressure drop over a transducer surface as a function of microscopic parameters of a transforming component:

$$\langle \delta p^2 \rangle_{\omega} = 2k_B T R_h, \quad (12)$$

where R_h is the transducer's hydrodynamic resistance, k_B is the Boltzmann constant, T is the absolute temperature, and ω is the frequency.

In the wide frequency range, the spectrum of MET self-noises is analogous to Nyquist noise except for the fact that, in the MET, R_h serves as an electric resistance. In the history of creation of METs, an important role was played by [35] because the technique for experimentally and theoretically estimating the intrinsic noises of certain devices was developed on their basis. Formula (25) was multiply confirmed experimentally for different types of practically used devices whose hydrodynamic resistance was $R_h \sim 10^9$ (Ns)/m⁵.

The experiments of [36–39] demonstrated that the dependence of transducer self-noises on the aforementioned parameters can be more complex than that corresponding to formula (12). In particular, it was established that, beginning with some level of an external signal, absolute noise is determined by its amplitude and the spectral density of MET noise increases toward low frequencies with decreasing hydrodynamic resistance.

At low frequencies, a substantial contribution to MET self-noises investigated in [35] is provided by hydrodynamic noise of the vortical pulsations of local velocities and pressure, which were studied in [37]. These pulsations arise when an electrolyte flow passes over the transducer's electrode system at sufficiently high signal level.

In the operating frequency band, the total spectral density of hydrodynamic noise of METs, which is expressed in acceleration units, has the form

$$\langle \delta a^2 \rangle_\omega = \frac{\sqrt[3]{2}}{432 (2\pi)^{8/3}} \left(\frac{R}{\xi} \right)^4 \left(\frac{Sa}{S_0} \right)^{2/3} \times \left(\frac{\xi \rho a}{S} \right)^{5/3} \frac{1}{l^{1/3} R_h^{8/3}} + \frac{2k_B T R_h}{\rho^2 l^2}, \quad (13)$$

where a is the disturbing signal (external acceleration), R is the characteristic size of the component of an electrode structure, ξ is the boundary layer thickness, S is the total area of holes in the grid electrode, S_0 is the cross-section area in the transducer channel, l is the transducer-channel length, and ρ is the electrolyte density.

Local vortical pulsations contribute substantially to total hydrodynamic noise starting with a level of $(1.5-3) \times 10^{-8} \text{ m/s}^2/\sqrt{\text{Hz}}$, and its value grows with increasing signal level.

The authors of [38, 39] investigated noises of the MET in the vertical seismosensor with fixed membranes at channel ends. This actually excluded an integral liquid flow in the channel and the influence of noise examined in [35]. It was demonstrated that, at frequencies lower than 0.1 Hz, the transducer with reduced hydrodynamic resistance R_h exhibits noise exceeding the Kozlov–Sakharov noise level [35] and growing toward low frequencies. In [39], the model describing the physics of appeared noise of the given type, which is related to closed microflows through separate channels in the dielectric partition between electrodes and nonidentical electron-grid components in each of these channels, was proposed.

The method of random forces made it possible to obtain the expression for the above-described model:

$$\langle v \rangle_\omega^2 = \beta \frac{4k_B T}{R_h} (\bar{k})^2 \alpha^2, \quad (14)$$

where \bar{k} is the averaged electrochemical transfer function of the transducer, β is the coefficient whereby the output noise current is transformed into input velocity units, $\alpha = \sqrt{\langle (\Delta k_n)^2 \rangle} / (\bar{k})^2$ is the semiempirical coefficient exhibiting the degree of inhomogeneity of an electrode mesh in the molecular-electronic cell, and Δk_n is the deviation of the flow-velocity transformation from the average value for the n th channel. In

the case of additional noise in the current, the following expression is valid:

$$\langle I^2 \rangle = 4k_B T N \left\langle \frac{(\Delta k_n)^2}{r_n} \right\rangle, \quad (15)$$

where N is the number of microchannels in the dielectric partition and r_n is the hydrodynamic resistance of the n th channel.

The influence of the given intrinsic-noise mechanism can be decreased by selecting the optimal parameters of an electrode mesh in the assembly. In this case, parameter α takes the smallest value [40].

The authors of [26] proposed the theoretical model of diffusion-current fluctuations in the molecular-electronic cell with planar electrodes under conditions that convection is free and an integral liquid flow is lacking in the channel with different Rayleigh numbers Ra . It was demonstrated that the convection noise can be diminished by decreasing the system's Rayleigh number, which can be attained by reducing an electrolyte concentration or the sizes of the components of a transforming cell. However, Ra cannot be very small because an increase in hydrodynamic resistance leads to a growth in hydrodynamic noise [35].

In [41], electronic noises specifying the operating transducer voltage and ensuring current transformation into an output voltage of the molecular-electronic cell were investigated. The practical problem in which the intrinsic noises of the MET is separated from noises introduced by corresponding electronics reduces to corrective determinations of transducer impedances. In turn, this is not always a trivial problem.

It was found that noises introduced by concomitant electronics and caused by the impedance of METs arrange at the input of the electronic cascade of signal amplification provide appreciable contribution only at frequencies of higher than 10–20 Hz and small concentrations: 0.002–0.01 mol/L. For all investigated samples, electronic noises lie substantially lower than the sensor self-noise at higher electrolyte concentrations and frequencies of 1–10 Hz. When the frequency exceeds 1 Hz, the intrinsic noise of MET-based measuring devices arises from convective processes in the transforming component, rather than concomitant electronic noises, as was regarded earlier.

The authors of [42] proposed the model of the intrinsic noises of molecular-electronic angular sensors operating at frequencies of 1–150 Hz. It was revealed from experimental data that convection noise satisfying the mechanism reported in [43] is prevailing in the frequency range of up to 50 Hz and noise related to the voltage of the input operational amplifier of a sensor's electronic block is predominant at higher frequencies. In this case, noise corresponding the latter of the given mechanisms depends on the output impedance of sensors. In [42], it was assumed that the impedance is purely active and the frequency depen-

dence of the impedance must be allowed for in the more accurate model.

Figure 5 illustrates the typical noise records of the MET presented in terms of the power spectral density. The cross-correlation method enables us to extract the correlated part from the signal records of two devices (curves 1 and 2), providing the result in the form of curve 3 corresponding to the noise characteristic of the MET.

In addition, let us consider the typical noise and dynamic characteristics of established classes of MET-based devices. The characteristic values of formed different classes of MET-based devices are summarized in Table 1 composed on the basis of the review presented in [44]. A large number of MET-based devices has been developed, and the Russian company “R-sensors” commercially produces seismometers, which successfully compete with the best foreign instruments in the world market [6, 7, 45–50].

5. REQUIREMENTS TO DEVICES AND MOLECULAR-ELECTRONIC TRANSDUCER APPLICATION IN SEISMOLOGY

The quality of seismic stations and the self-noise level of seismic devices were estimated using the Peterson low-noise model (LNM) [51, 52] and the high-noise model (HNM). To construct models, a certain characteristic describing the frequency distribution of noises (e.g., spectral densities) for a large number of seismic stations, which was recorded during the calm period of the given stations, was chosen. Afterward, envelopes from above (HNM) and from below (LNM) are constructed for the obtained set of curves. Subse-

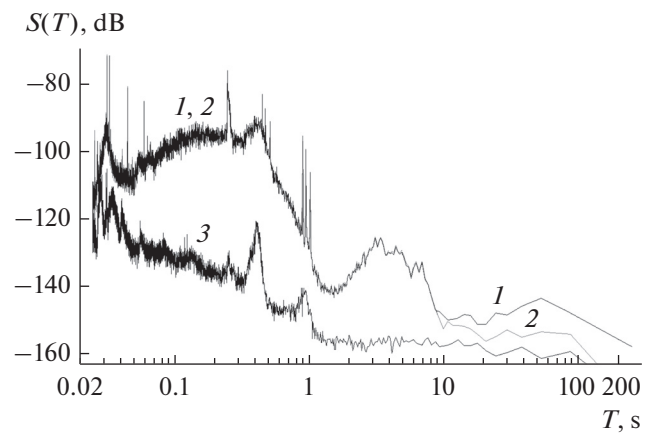


Fig. 5. Power spectral densities of the MET-based miniature geophone. Curves 1 and 2 were recorded during long signals or two identical geophones, and curve 3 corresponds to the intrinsic-noise level calculated via the cross-correlation method.

quently, owing to accumulation of a large amount of experimental data, the new low-noise model (NLNM) appeared.

In many cases, almost everywhere observed noise exceeds the LNM by a rather perceptible value. For example, at frequencies of higher than 1 Hz, the noise level greater than the NLNM by 20 dB can be assumed as uniquely low. Another example is microseism noise between 2 and 20 s, which has strong seasonal variations and can be up to 50 dB higher than the NLNM in the winter period. At low frequencies, the noise level is distinguished by a large stability and is commonly 10–20 dB higher than the LNM even for places

Table 1. Typical noise and dynamic characteristics of different classes of MET-based devices

Device class	Device characteristics			
	self-noise level	self-noise value	maximum recorded signal	dynamic range, dB
Wideband seismometers	–130 to –160 dB (from the level of 1 m/s ² √Hz)	10 nm/s ² √Hz	±7.5 mm/s	125
Short-period seismometers	–140 dB (from the level of 1 m/s ² √Hz)	15 nm/s in the operating band	[±3.75 mm/s ± 7.5 mm/s]	120
Compact seismosensors	–120 dB (from the level of 1 m/s ² √Hz)	100 nm/s 70 ng/√Hz at 10 Hz	50 mm/s at 100 Hz	110
Strong motion accelerometers	–110 to –120 dB (from the level of 1 m/s ² √Hz)	130 hg/√Hz, at 10 Hz	±0.8 g/±4 g	130
Angular seismosensors	–122 dB (from the level of 1 m/s ² √Hz)	8 × 10 ^{–7} rad/s ² √Hz 2 × 10 ^{–7} rad/s planar in the range of 0–10 Hz	±0.1 rad/s	110

Here and in Table 3, 1 ng = 9.81 × 10^{–9} m/s².

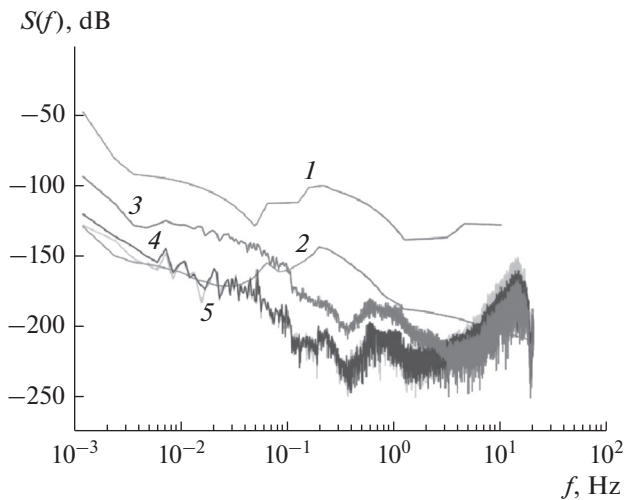


Fig. 6. Comparison between the self-noises of seismometers: curve 1 corresponds to the Peterson LNM [53], curve 2 is the HNM, curve 3 is the self-noise of the R-sensors SME-6211 seismometer based on the MET, curve 4 is the self-noise of the Shtreckeisen ST62 seismometer, and curve 5 is the self-noise of the Trillium T240 seismometer.

that are noisy in other relations. The latter statement is valid only for a vertical channel for which the model was constructed. In the case of horizontal components, the noise level corresponding to frequencies of lower than 0.05 Hz is tens of decibels higher and undergoes strong changes. This can be attributed to the fact that horizontal channels are strongly sensitive to inclinations created by wind loads on closely spaced trees and buildings. Another source of such inclinations is atmospheric-pressure variations along the Earth surface.

Thus, when the device self-noise is lower than the Peterson model, such device is applicable to recording of very weak signals at exceptionally calm seismic stations. The devices whose noises are 10–20 dB higher than the NLNM can be used at the majority of seismic stations. An CME-6211 seismometer [53] refers to such a class of devices. This determines its high relevance in practice. For widespread seismometer models, the self-noise levels with respect to the NLNM and HNM is depicted in Fig. 6.

At the same time, devices with higher noises can be employed in seismic measurements to record rather strong motions of the Earth surface. CME-4211 and CME-4311 models have found wide application under field conditions, where the noise level is appreciably higher than that inherent to seismic stations used to construct the noise model described above. Hence, the first place occupies performance criteria, such as a small mass and compact sizes in combination with reliability and simple utilization [54].

In [55], the calderas of volcanos belonging to the Avachinskaya group (Kamchatka) were investigated. Continuous measurements were performed during

several months by means of the time network involving 11 seismic stations equipped with CME-4311 instruments. Afterward, with the help of 21 analogous seismic stations, the Gorelyi volcano model was constructed.

In [56], MTSS-2003 seismoreceivers based on the molecular-electronic principle of operation were employed to record soil oscillations of the subgrade and the peat roadbed of railway lines during train motion.

The SEHELLARC Greek project on the creation of terrestrial-underwater seismic network with real-time data transmission for early prediction of tsunamis, the composition of which incorporates terrestrial and bottom stations equipped with MET-based CME-4011 devices in standard modification and that for bottom seismic stations, is efficiently developed [57–59]. Details concerning the application of MET-based seismometers included in bottom seismic stations can be found in [60, 61].

Three digital regional seismic stations equipped with CME-6011 and CME-4011 devices in the low-temperature modification operate in the YARS seismic network located at Sakha (Yakutia) republic (regional codes and station names are VTM (Vitim) operating continuously since 2003, BLS (Bulus), and SOT (Stolb) placed in the zone of perpetual congelation) [62].

Moreover, CME-4111 seismometers were used to monitor the ice-field state in the day and night recording mode and investigate the dynamic properties of sheets of ice at drifting stations North Pole-36, North Pole-39, and North Pole-40. The same seismometer model was employed to observe the dynamics of the Nordenskjöld Glacier via the seismometric method [63].

At present, MET-based seismometers occupy a confident position in the world market and enable the obtainment of scientific data of new quality. However, the potential of MET application in measuring instruments is not exhaust by seismological equipment. Nowadays, the development of microelectronic technologies of MET manufacturing moves the technological restrictions imposed on METs toward upper operating frequency and creates the opportunities mass production, thereby extending the circle of possible applications of sensors based on them.

6. DEVICES AND SYSTEMS BASED ON PLANAR AND MESH MOLECULAR-ELECTRONIC TRANSDUCERS

The modern state of MET-based instrument engineering was described in [64, 65]. Seismometers, accelerometers, and geophones based on METs are commercially produced by Russian research-and-production companies R-sensors [44], Seismotronics [66], and NordLab [67] created by graduates of the Moscow Institute of Physics and Technology (MIPT)

Table 2. Comparative characteristics of MET-based single-component geophones and those of widespread geophones of other manufacturers

Geophone parameters	Manufacturer and geophone name			
	OOO Geospace, GS-11D	Sercell, L28LB	R-sensors, MTSS-1001	Seismotronics, STRA-1001
Sensing-element type	Magnetomechanical	Magnetomechanical	MET	planar MET
Number of axes	1	1	1	1
Height, mm	34	38	35	50
Diameter, mm	32	31	32	32
Lower boundary frequency, Hz	4.5, 8, 10, 14 ± 0.75	4.5	1 ± 0.05	1 ± 0.05
Transformation coefficient, V/m/s	32 ± 10%	31.3	250 ± 2%	250 ± 1%
Nonlinear-distortion coefficient, % at a signal of 18 mm/s/measurement are performed at 12 Hz	<0.2 for versions with 8 Hz, 10 Hz, 14 Hz (nonspecified for version 4.5 Hz)	<0.2	<0.1	<0.2
Requirements to determination	Inclination angle of <30°	There no indications	0 perability at any orientation	0 perability at any orientation

(State University) and (or) with the participation of the MIPT. Technical characteristics of commercial devices are presented at the sites of the given companies. A number of works was devoted to the study of MET characteristics and application of seismometers and geophones [68–71].

It should be emphasized that the development of the methods whereby the temperature dependence is simulated [72] made it possible to create the efficient methods for temperature derating compensation. Since the feedback was introduced into the device structure, the problem concerning the frequency correction of device characteristics was solved to a great extent [45].

On the basis of the new planar MET, the prototype of a high-accuracy geophone was produced and its characteristics were investigated. The main results are presented in [6, 7]. The new type of high-accuracy geophones appeared in the market of seismic prospecting devices can exert considerable complex influence on the efficiency of seismic works in the part of their acceleration, cost reduction, resolution improvement, and an increase in exploring depth. MET-based geophone characteristics are compared with those of single-component magnetomechanical geophones and three-component MEMS-based ones in Tables 2 and 3.

Single- and multicomponent recorders of rotational motions are also commercially produced [72, 73]. They have a special importance due to grow-

ing interest in the investigations of the rotational component of a seismic field. In 2006, International Working Group on Rotational Seismology (IWGoRS) [74] was created to study all aspects of rotational motion in the seismology field. In particular, recording of the ratio between the amplitudes of linear and angular oscillations, which is performed using a six-component seismoreceiver, makes it possible to estimate source sizes and more accurately extract transverse waves. With the use of six-component seismometer network, it is possible to highly accurately determine epicenter coordinate [75]. The necessity of studying the rotational oscillations of the Earth surface and possible directions of investigations were discussed in [76].

Rotational sensors can also be employed in the monitoring system of the state of complex engineering objects, such as bridges, dykes, dams, and high-rise buildings. Comparative characteristics of MEMS-based sensor of rotational motion and those of other types of sensors are presented in Table 4. The high accuracy of electrochemical rotation sensors enabled the development of original navigational devices to determine the direction to the geographical pole [77] via inertia methods. As was demonstrated, determining the amplitude and phase of the signal rotating in the Earth gravitational field around the vertical rotation axis, it is possible to find the projection of the Earth rotation velocity on the given latitude and the

Table 3. Comparative characteristics of MET-based three-component geophones and those of certain three-component geophones of other manufacturers

Geophone parameters	Manufacturer and geophone name			
	R-sensors and Seismotronics, commercial MTSS-1033A	Seismotronics, plamar STRA-1030/STRA-1010	ION, seisoaccelerometer Colybrys Digital-3 used in the Vectorseis system	Shell + Hewlett-Packard, developments are performed jointly
Measured signal range, m/s^2	± 30 (at any inclination), overloading is excluded under operation conditions	± 30 (at any inclination), overloading is excluded under operation conditions	± 3.3 (at any inclination). The time of recovery of operability under overloading is ~ 1 s	There are no data
Noise, ng/\sqrt{Hz}	~ 45	~ 20	~ 45	~ 10
Frequency range, Hz	0.1–120	1–500	DC (1450_)	DC (0.1–1000)
Dynamic range, dB, in the band of up to 100 Hz	135	130	120	There are no data
Nonlinear distortions, %, at 12 Hz under the condition that peak-to-peak input signal is 18 mm/s	± 0.05	± 0.01	± 0.002	There are no data

Table 4. Comparative table of different angular sensors of motion

Sensor parameters	Manufacturer and sensor name				
	Sensoron, STIM210	Columbia Research Laboratories, SR100FR	Emcore, EMP-1.2K	Fizoptica VG 910	R-sensors, METP-03
Principle of operation	Shift of vibrating inertial mass under the action of Coriolis force, MEMS technology	Toroidal channel filled with liquid and the piezoelectric transducer of pressure and liquid drops	Fiber-optical gyroscope	Fiber-optical gyroscope	MET-based transducer
Self-noise level, $rad/s/\sqrt{Hz}$	5×10^{-5}	3×10^{-5}	5×10^{-7}	1.5×10^{-5}	3×10^{-8}
Component price, US dollars	>1000	>1000	>10000	>2000	~ 500

direction to the geographical North pole coinciding with the maximum of the recorded projection of the Earth rotation velocity.

The opportunity of recording a constant linear acceleration was previously assumed to be substantial advantage of MEMS accelerometers over electrochemical systems. To solve this problem, the new structure of an electrochemical transducer with an efficient inertia mass created by means of electrochemical methods, which was capable of measuring a constant linear acceleration, was proposed [78]. However, this construction has a comparatively high level

of intrinsic noises. To preserve acceptable noise levels, combined (MEMS + MET) low-noise sensors, which joined the advantages of MEMS and MET technologies, were developed [79, 80]. For this purpose, summation of signals from both sensors was employed. Moreover, the frequency band of each sensor was restricted so that the amplitude characteristic obtained after summation would an independent form in frequency. In this case, MEMS accelerometer whose noise level is much higher than that of the MET accelerometer at medium and high frequencies provides information on the signal only at frequencies

from zero to hundredths of a hertz. All other frequency range is covered by the MET-accelerometer signal. Owing to the addition of the narrowband MEMS-accelerometer signal, the combined device can record a combined component of acceleration. Since the band of a MEMS signal becomes narrow as compared to the frequency band of the combined device, its noise additive is insignificant and resultant noise parameters of the combined device remain practically identical to those of the single MET.

At present, several tens of original experimental devices and systems intended for the solution of various problems have been developed in the Department of Physical and Quantum Electronics of the MIPT at the Center of Molecular Electronics based on MET technology, among which can be distinguished, e.g., the system of personal inertial navigation of foot-passengers [81], the system of monitoring of high-rise building oscillations [82, 83], the seismic security system of foreign type making it possible to record the “violator” motion trajectory [84], and the meter of the rotational oscillations of the Earth surface during the remote control of the boring process [85].

Motion-parameter meters based on molecular-electronic transfer in METs have a rather wide sphere of application under the conditions of their low prime cost upon mass production with the help of modern microelectronic technologies and quantitative enhancement in technical parameters. This comprises (2D and 3D, including vectorial) seismic prospecting, navigation systems, including portable, personal, and intended for small autonomously acting devices, systems of vibrocontrol and seismic monitoring of the states of buildings and constructions, certain medical applications (portable cardiomonitoring systems, orthopedics, and sport medicine), car security systems, and robotics. Aggregation of the advantages of signal’s electrochemical recording and microelectronic technologies can lead to the creation of the new class of microelectronic devices.

ACKNOWLEDGMENTS

This study was supported by the Russian Foundation for Basic Research, project no. 18-07-01162.

REFERENCES

1. *Introduction to Molecular Electronics*, Ed. by N.S. Lidorenko (Energoatomizdat, Moscow, 1984) [in Russian].
2. V. S. Borovkov, B. M. Grafov, E. M. Dobrynin, et al., *Electrochemical Transducers of Primary Information*, Ed. by E. M. Dobrynin and P. D. Lukovtsev (Mashinostroenie, Moscow, 1969) [in Russian].
3. J. Newman and K. E. Thomas-Alyea, *Electrochemical Systems* (Wiley, Hoboken, 2004).
4. C. W. Larkam, *J. Acoust. Soc. Am.* **37**, 664 (1965).
5. V. M. Agafonov, V. G. Krishtop, and M. V. Safonov, *Nano & Mikrosist. Tekh.* **5** (6), 47 (2010).
6. A. S. Bugaev, V. M. Agafonov, V. G. Krishtop, A. N. Antonov and V. S. Veretin, “Seismic sensors for oil and gas complex on the molecular-electronics transduction in the solid state and liquid microsystems,” *Oil & Gas Field Engineering, Special Issue No. 3: Results of 2012*, 46–52 (2013) Issue, Results.
7. V. M. Agafonov, V. G. Krishtop, and I. V. Egorov, *Devices & Syst. of Explor. Geophys.* **43** (1), 39 (2013).
8. V. G. Krishtop, V. M. Agafonov, and A. S. Bugaev, *Russ. J. Electrochem.* **48**, 746 (2012).
9. I. S. Zakharov, V. A. Kozlov, and M. V. Safonov, *Izv. Vyssh. Uchebn. Zaved., Elektron. No. 2*, 40 (2003).
10. I. S. Zakharov and V. A. Kozlov, *Russ. J. Electrochem.* **39**, 397 (2003).
11. V. M. Agafonov and V. G. Krishtop, *Mikrosistem. Tekh.*, No. 9, 40 (2004).
12. V. M. Agafonov and V. G. Krishtop, *Russ. J. Electrochem.* **40**, 537 (2004).
13. V. A. Kozlov and P. A. Tugaev, *Russ. J. Electrochem.* **32**, 1325 (1996).
14. A. V. Babanin, V. A. Kozlov, and N. V. Pet’kin, *Russ. J. Electrochem.* **26**, 601 (1990).
15. V. A. Kozlov, A.S. Korshak, and N. V. Pet’kin, *Russ. J. Electrochem.* **27** (1), 25 (1991).
16. I. S. Zakharov, *Russ. J. Electrochem.* **40**, 626 (2004).
17. V. A. Kozlov and D. A. Terent’ev, *Russ. J. Electrochem.* **39**, 401 (2003).
18. V. A. Kozlov and D. A. Terent’ev, *Russ. J. Electrochem.* **38**, 992 (2002).
19. V. A. Kozlov and M. V. Safonov, *Russ. J. Electrochem.* **40**, 460 (2004).
20. I. S. Zakharov, *Avtonom. Energetika*, No. 15, 36 (2003).
21. I. S. Zakharov, *Avtonom. Energetika*, No. 13, 23 (2002).
22. V. M. Agafonov and A. A. Orel, *Nano & Mikrosist. Tekh.*, No. 5, 50 (2008).
23. V. M. Agafonov, A. S. Bugaev, and A. A. Orel, *Nano & Mikrosist. Tekh.*, No. 5, 32 (2009).
24. V. M. Volgin and A. D. Davydov, *Russ. J. Electrochem.* **48**, 565 (2012).
25. M. R. Vyaselev, A. G. Miftakhov, and E. I. Sultanov, *Russ. J. Electrochem.* **38**, 208 (2002).
26. M. V. Safonov, *Issledovano v Rossii*, 2433 (2004), [Elektron. Zh.]. <http://zhurnal.ape.relarn.ru/articles/2004/228.pdf>.
27. D. A. Bograchev and A. D. Davydov, *Electrochim. Acta* **47** (20), 3277 (2002).
28. B. M. Grafov, *Russ. J. Electrochem.* **3**, 935 (1967).
29. N. S. Lidorenko, *Elektrotekhnik*, No. 3, 13 (1965).
30. S. A. Martem’yanov, M. A. Vorotyntsev, and B. M. Grafov, *Russ. J. Electrochem.* **16**, 714 (1979).
31. A. P. Grigin, B. I. Il’in, and N. V. Pet’kin, *Russ. J. Electrochem.* **15**, 1 (1980).
32. V. A. Kozlov and D. A. Terent’ev, *Mikrosistem. Tekh.*, No. 10, 41 (2004).

33. E. Ya. Klimenkov, B. M. Grafov, V. G. Levich, and I. V. Strizhevskii, *Russ. J. Electrochem.* **5**, 202 (1969).
34. V. G. Krishtop and A. S. Shabalina, in *Proc. XLVI Sci. Conf. MIPT, Dolgoprudnyi, 2003* (MIPT, Dolgoprudnyi, 2003), p. 43.
35. V. A. Kozlov and K. A. Sakharov, *Basic Physics of Fluid and Solid-State Measuring Systems and Information-Processing Devices* (MIPT, Moscow, 1994), p. 37.
36. M. V. Safonov, *Convection Diffusion and Noise in Molecular-Electronic Structures*, Cand. Sci. (Phys. Math.) Dissertation (MIPT, Dolgoprudnyi, 2007).
37. V. A. Kozlov and M. V. Safonov, *Tech. Phys.* **48**, 1579 (2003).
38. D. L. Zaitsev, P. V. Dudkin, and V. M. Agafonov, *Izv. Vyssh. Uchebn. Zaved., Elektron.*, No. 5, 61 (2006).
39. D. L. Zaitsev and P. V. Dudkin, *Avtonom. Energetika*, No. 19, 62 (2005).
40. V. A. Kozlov, V. M. Agafonov, D. L. Zaitsev, and M. V. Safonov, RF Patent No. 2394246 *Byull. Izobret.*, No. 19 (July 10, 2008).
41. Yu. V. Klyus and M. V. Safonov, in *Contemporary Problems of Fundamental and Applied Sciences (Proc. XLIX Sci. Conf. MIPT, Moskva–Dolgoprudnyi, 2006)* (MIPT, Dolgoprudnyi, 2006), p. 100.
42. E. V. Egorov, I. V. Egorov, and V. M. Agafonov, *J. Sensors* **2015** ID 512645 (2015).
43. V. M. Agafonov and D. L. Zaitsev, *Tech. Phys.* **55**, 130 (2010).
44. <http://www.r-sensors.ru>.
45. V. M. Agafonov, I. V. Egorov, and A. S. Shabalina, *Seismic Instruments* **49**, 5 (2013).
46. E. Son, V. Agafonov, A. Bugaev, and V. Krishtop, in *Proc. ASME 2nd Micro/Nanoscale Heat & Mass Transfer Int. Conf. (MNHMT 2009), Shanghai, China, Dec. 18–21, 2009* (Am. Soc. Mech. Engineers, New York, 2009).
47. I. P. Kasperovich and V. G. Krishtop, in *Components of Domestic Radio Electronics (Proc. 1st Russian-Byelorussian Sci.-Tech. Conf., Nizhny Novgorod, Sep. 11–14, 2013)* (Popov RNTO RES, Moscow, 2013), Vol. 1, p. 28.
48. A. S. Bugaev, V. M. Agafonov, M. S. Khairtdinov, and V. V. Kovalevskii, in *Nigmatullin's Readings (Proc. Int. Sci.-Tech. Conf., Kazan, Nov. 19–21, 2013)* (Kazan. Gos. Tekh. Univ., Kazan', 2013), p. 213.
49. V. M. Agafonov, A. S. Bugaev, V. G. Krishtop, et al., in *Actual Problems in Geosciences (Proc. Russian-Polish Workshop, Oct. 15–16, 2008)* (Schmidt Inst. of the Earth Physics, RAS, Shirshov Inst. of Oceanology, RAS, Moscow, 2008), p. 15.
50. A. S. Shabalina and V. G. Krishtop, "The precision seismometer based on planar molecular-electronic transducers," in *Nigmatullin's Readings (Proc. Int. Sci.-Tech. Conf., Kazan, Nov. 19–21, 2013)* (Kazan. Gos. Tekh. Univ., Kazan', 2013), p. 183.
51. J. Peterson, *Observation and Modeling of Seismic Background Noise. Open File Report*, 93–322 (Albuquerque: US Dept. of Interior Geological Survey, Albuquerque 1993). <https://pubs.er.usgs.gov/publication/ofr93322>.
52. E. Wielandt, *The New Manual of Seismological Observatory Practice (NMSOP-2)*, Ed. by P. Bormann (Deutsches GeoForschung Centrum GZF, Potsdam, 2012), Ch. 5. http://gfzpublic.gfz-potsdam.de/pubman/item/escidoc:56076:4/component/escidoc:61055/Chapter_5_rev1.pdf.
53. *Programm for Array Seismic Studies of the Continental Lithosphere (PASSCAL)*. N.Y.: Incorporate Research Institution for Seismology (IRIS), 2008). https://www.iris.edu/hq/files/publications/passcal_review.pdf.
54. M. E. Templeton, *IRIS Library of Nominal Response for Seismic Instruments. Incorporated Research Institutions for Seismology. Dataset* (IRIS, Washington, 2017). <https://doi.org/doi.10.17611/S7159Q>
55. I. Koulakov, K. Jaxybulatov, N. M. Shapiro, et al., *J. Volcanology & Geothermal Res.* **285**, 36 (2014).
56. A. F. Kolos and D. V. Kryukovskii, *Izv. Peterburg. Gos. Univ. Putei Soobshch.*, No. 2, 120 (2013).
57. J. M. Akris and A. T. Sambas, *Bollettino di Geofisica Teorica ed Applicata* **55**, 561 (2014).
58. J. Papoulia, J. Makris, D. Ilinski, et al., in *Proc. 9th Hellenic Symp. of Oceanography and Fisheries, Patra, May 13–16, 2009* (Hellenic Center for Marine Research, Athens, 2009), Vol. 1.
59. J. Papoulia, R. Nicolich, J. Makris, et al., *Bollettino di Geofisica Teorica ed Applicata* **55**, 405 (2014).
60. D. G. Levchenko, *Seismic Instruments* **45** (4), 5 (2009).
61. D. G. Levchenko, *Recording of Broadband Seismic Signals and Possible Strong Foreshocks on the Bottom of the Sea* (Nauchnyi Mir, Moscow, 2005).
62. <http://eqru.gsras.ru/stations/index.php?inc=netlist>.
63. V. G. Korostelev, L. M. Savatyugin, and V. N. Smirnov, *Problemy Arktiki i Antarktiki*, No. 3 (101), 69 (2014).
64. V. A. Kozlov, *Achievements of Modern Radioelectronics*, Nos. 5–6, 138 (2004).
65. A. S. Shabalina, D. L. Zaitsev, E. V. Egorov, et al. *Achievements of Modern Radioelectronics*, No. 9, 33 (2014).
66. <http://www.seismotronics.ru>.
67. <http://www.nordlab.com>.
68. D. Zaitsev, V. Agafonov, E. Egorov, and A. Antonov, and A. Shabalina, *Sensors.*, No. 11, 29378 (2015).
69. E. V. Egorov, V. A. Kozlov, and A. V. Yashkin, *Russ. J. Electrochem.* **43**, No. 12, 1358 (2007).
70. V. A. Kozlov and M. V. Safonov, *Russ. J. Electrochem.* **40**, 460 (2004).
71. V. M. Agafonov and A. S. Nesterov, *Russ. J. Electrochem.* **41**, 880 (2005).
72. V. G. Krishtop, *Russ. J. Electrochem.* **50**, 350 (2014).
73. V. M. Agafonov, K. A. Afanas'ev, A. N. Nikolaev, and A. V. Yashkin, *Novye Prom. Tekhnol.*, No. 6, 68 (2010).
74. <http://www.rotational-seismology.org/>.
75. W. H. K. Lee, H. Igel, and M. D. Trifunac, *Seismological Research Lett.* **80**, 479 (2009).

76. W. H. K. Lee, J. R. Evans, B.-S. Huang, et al. *The New Manual of Seismological Observatory Practice (NMSOP-2)*, Ed. by P. Bormann (Deutsches GeoForschung Centrum GZF, Potsdam, 2012). http://gfzpublic.gfz-potsdam.de/pubman/item/escidoc:43316:3/component/escidoc:56116/IS_5.3_rev1.pdf.
77. A. M. Agafonov, E. V. Egorov, D. L. Zaitsev, et al., *Giroskopiya i Navigatsiya*, No. 3 (70), 14 (2010).
78. A. M. Agafonov, E. V. Egorov, and D. L. Zaitsev, *Giroskopiya i Navigatsiya*, No. 1(68), 72 (2010).
79. A. Neeshpapa, A. Antonov, and V. Agafonov, *Sensors* **15**, 365 (2015).
80. A. N. Antonov and D. L. Zaitsev, *Giroskopiya i Navigatsiya*, No. 2(69), 63 (2010).
81. D. L. Zaitsev and A. M. Panteleev, *Giroskopiya i Navigatsiya*, No. 2(65), 103 (2009).
82. N. Kapustian, G. Antonovskaya, V. Agafonov, et al., *Seismic Behaviour and Design of Irregular and Complex Civil Structures*, Ed. by M. De Lavan, M. De Lavan, (Springer-Verlag, Dordrecht, 2013), p. 353.
83. N. K. Kapustyan, G. N. Antonovskaya, and A. N. Klimov, "Monitoring of high-rise buildings as an important asset for the construction design," *Zhishchnoe Stroitel'stvo (Housing Construction)*, No. 11, 6 (2013).
84. A. M. Agafonov, K. A. Afanas'ev, and A. V. Yashkin, *Proc. of MIPT* **5** (2/18), 142 (2013).
85. V. A. Kozlov, V. M. Agafonov, and P. V. Dudkin, in *System Problem of Reliability, Quality, Information and Electronic Technologies (Proc. Int. Sci.-Tech. Conf., Moscow, Oct. 3–14, 2005)* (Radio i Svyaz', Moscow, 2005), p. 142.

Translated by S. Rodikov